NPL EL/TM/20

INVESTIGATION OF POSSIBLE INFLECTION SYSTEMS

by

I. I. Rabinowitz

National Institute for Research in Nuclear Science,
Daresbury Nuclear Physics Laboratory,
Daresbury,
Warrington.

INFLECTOR IN SHORT STRAIGHT

INTRODUCTION

Report EL/TM/17 gives the reasons for investigating this inflection system, in which, with the NINA magnet lattice and focussing order, the beam enters the synchrotron in a long straight and passes through the stray field of a D-magnet before reaching the inflector centred on the middle of a short straight (Figure 1). This report summarises the effect of the stray field on the beam.

Report EL/TM/18 gives the distribution of apertures and inflection parameters for electron and positron beams with and withour bunching. From this we take the maximum radial and vertical acceptances of the synchrotron to be 23 x 10^{-6} mrad, (2.3 cm mrad) and the maximum momentum deviations in the injected beam to be $\pm$ 1.65%.

An initial calculation showed that a particle with momentum deviation of - 1.65% starting on its displaced equilibrium orbit in the synchrotron would have, working backwards, a displacement of just under 20 cm at the end of the long straight after passing through an inflector of angle 20 mrad (for a particle with synchronous momentum) and through the D stray field. This is around the clearance of the F magnet we require and we therefore consider an angle of 20 mrad.

The problem is essentially to trace particle paths through the D stray field. The method used is to assume an ideal beam transport and momentum matching system. We can then take ideal paths leaving the inflector and trace them backwards through the inflector and D stray field. A Mercury Autocode programme has been written which analyses both the radial and vertical motion through the D stray field.

METHOD AND DETAILS OF CALCULATION

Radial Motion

Consider a particle of momentum p entering a magnet physically similar to the ideal synchrotron magnet but with a uniform field B, with initial radial deviation and angular deviation A and α relative to the ideal orbit (Figure 2). The particle will describe an arc of a circle, radius

$$\rho = \rho_o \frac{B_o}{B} \quad \frac{p}{p_o}$$

where B_o is the field required to move a particle of synchronous momentum p_o on the ideal path, radius ρ_o. With O as the origin of an XY co-ordinate system, the centre of the circle radius ρ will be $P(X_o, Y_o)$ where

$$X_o = (\rho_o + A) - \rho \cos \alpha$$
$$Y_o = \rho \sin \alpha \ .$$

Relative to O the equation of the circle will be

$$(x - X_o)^2 + (y - Y_o)^2 = \rho^2$$

which, substituting with polar co-ordinates r, θ gives

$$r(\theta) = X_o \cos \theta + Y_o \sin \theta + \rho \cos \phi (\theta) \qquad (1)$$

where

$$\phi (\theta) = \sin^{-1} \left\{ \frac{Y_o \cos\theta - X_o \sin\theta}{\rho} \right\} \qquad (2)$$

$\phi(\theta)$ is the angular deviation of the path from the ideal path at angle θ. (1) and (2) thus enable us to find the radial deviation and angular deviations of the path from the ideal orbit at angle θ, or more important in this case, enable us to calculate θ and $\phi(\theta)$ when the radial displacement has reached a certain value. This is the basis of the radial path tracing.

The magnet median plane of the D is divided into arc strips of small width (Figure 3), inside which the vertical field (i.e. the field normal to the plane) B_z is assumed uniform and equal to the mean field across the width. The initial displacement and angular displacement of a path at the beginning of the D are calculated (for determination of these see below) and the strip in which the displacement lies is found. The instantaneous ρ and thus X_o and Y_o are calculated and the step in θ, $\Delta\theta$, needed to bring the path to the edge of the strip is determined by a reiteration process. The displacement of the edge of the strip and $\phi(\Delta\theta)$ then become A and α for the next strip. This is continued until $\Sigma \Delta\theta = \theta_m$, the angle subtended by the magnet.

Vertical Motion

For computation of the radial motion the median plane of the D was divided into arc strips of uniform vertical magnetic field. However, vertical focussing effects are only produced by a non-uniform field and so we must look at the real nature of the D magnetic field.

When plotted on an expanded scale the theoretical plot of the vertical field on the median plane against radial displacement is seen to be divisible into a number of regions of constant gradient, i.e. regions in which dB_z/dr is very well constant. Table 1 gives the radial positions of these regions, the gradients in the regions and also the n values vorresponding to these gradients, where n is defined by

$$n = - \frac{r_o}{B_o} \frac{dB_z}{dr} \quad .$$

In the ideal magnet there is no azimuthal component of the field and the radial and vertical fields are independent of azimuth. The condition that curl $\underline{B}$ be zero then reduces to

$$\left.\frac{\partial B_r}{\partial z}\right|_r = \left.\frac{\partial B_z}{\partial r}\right|_r \quad .$$

In the linear theory the gradient of the field which affects the vertical motion (B_r) is assumed constant across the vertical aperture. Here we assume it is constant for the height of the vertical oscillations. The vertical oscillations in a region will then be simple harmonic, the wavelength and amplitude depending on the value of n in the region. Given initial conditions the motion may be calculated for a region of constant n by normal matrix methods. This is the basis of the calculation of the vertical motion.

The edges of some of the arc strips used in the radial calculations are arranged to be the radial position where changes in gradient take place. The path lengths between these discontinuities are calculated from knowledge of the radial lengths and steps in θ produced in the radial calculations. These lengths (and the appropriate n values) are used to produce a transfer matrix for each region, and a transfer matrix for the whole D magnet is produced by multiplication.

This final matrix is analysed to give the effect of the stray field on the vertical motion about the particular radial path. It is apparent that the vertical motion will vary with radial path. This is one of the effects we are investigating.

CALCULATION OF INITIAL RADIAL DEVIATIONS AT ENTRANCE TO D

Phase space contributions

The betatron oscillation amplitude functions, the β functions, for the radial and vertical directions give the orientations and shapes of the acceptance ellipses at any point in the magnet lattice. The sizes of the ellipses are of course dependent on the acceptances. The ellipses at any point transform themselves into the ellipsos at any other point on moving towards that point.

Moving in the direction of the reversed beam, the ellipses at the end of the F magnet previous to the inflector (Figure 1) transform themselves, in the normal case, to those at the beginning of the D by traversing the short straight. We require to see the effect the inflector has on these ellipses.

We deal here only with particles with synchronous momentum. The radial transfer matrix for an inflector with uniform vertical magnetic field is

$$\begin{bmatrix} \cos\phi & \frac{\ell}{\phi}\sin\phi \\ -\frac{\phi}{\ell}\sin\phi & \cos\phi \end{bmatrix} \equiv \begin{bmatrix} \cos\phi & \rho\sin\phi \\ -\frac{1}{\rho}\sin\phi & \cos\phi \end{bmatrix} \qquad \phi = \frac{\ell}{\rho}$$

where ℓ is the length of the inflector and ρ is the radius of curvature of the paths in the inflector. ϕ is then the inflector angle. This matrix gives the oscillations about the path of a particle which started on the equilibrium orbit.

If ϕ is small, so that $\cos\phi \simeq 1$ and $\sin\phi \simeq \phi$, the matrix becomes (neglecting $-\ell/\rho^2$ which is also small)

$$\begin{bmatrix} 1 & \ell \\ 0 & 1 \end{bmatrix} .$$

This is the transfer matrix for a length ℓ of straight. Thus the inflector, apart from deviating all the particles by the deviations produced on the central path, acts exactly like the free space it has replaced. The radial phase ellipse

at the beginning of the D will thus be the normal one but with its centre shifted in phase space. The centre of the phase ellipse for particles with synchronous momentum at the beginning of the inflector would be defined by the synchrotron orbit. In this case the centre of the ellipse at the D would be defined only by the deviations produced on the central path at the D by the inflector.

For a particle with non-synchronous momentum the centre of the phase ellipse prior to the inflector would be defined by the deviations of its displaced equilibrium orbit at that point. The centre of the ellipse at the D will then be defined by the sum of the deviations produced by the inflector and of the deviations of the displaced orbit, at the D.

Inflector contributions

If the inflector, length ℓ, moves particles with synchronous momentum on paths of radius ρ, such a particle which started on the synchrotron orbit will leave the inflector and arrive at the D with an angular deviation of $\alpha = \ell/\rho$. If α is small the deviation of the path at the end of the inflector will be $\alpha.\ell/2$, and if the inflector is centred on the middle of the short straight the deviation at the D will be $\alpha L/2$ where L is the length of the short straight. Thus the centre of the radial phase ellipse at the D for particles with synchronous momentum will be defined by

$$r = \alpha L/2 = 0.02 \cdot 50 = 1 \text{ cm}$$

$$r' = \alpha = 20 \text{ mrad.}$$

The effect of the inflector is momentum dependent. The deviations produced at the D on the central path of the phase ellipse for particles of momentum p will be given by

$$r_1 = \frac{p_o}{p} r \approx r \left\{ 1 - \frac{\Delta p}{p_o} \right\} \qquad p = p_o + \Delta p \qquad (3)$$

$$r_1' = \frac{p_o}{p} r' \approx r' \left\{ 1 - \frac{\Delta p}{p_o} \right\} \qquad (4)$$

Displaced equilibrium orbit contributions

The displaced equilibrium orbit for a particle with momentum p at the D is defined by

$$r_2 = 1.393\ \Delta p/p_o \text{ cm} \qquad \text{where } \Delta p = p - p_o \tag{5}$$

$\Delta p/p_o$ is expressed as a percentage

$$r_2' = -3.43\,\Delta p/p_o \text{ mrad} \quad . \tag{6}$$

The initial radial displacements operated on by the programme are then calculated as follows:

1. For a series of values of $\Delta p/p_o$ in the range $-1.65\% \leq \Delta p/p_o \leq +1.65\%$ the central displacements of the phase ellipse at the D are calculated from (3), (4), (5) and (6)

$$r_o = r_1 + r_2$$

$$r_o' = r_1' + r_2' \quad .$$

2. A number of points on the radial phase ellipse at the D are selected. These are shown in Figure 4. (The deviations shown are those relative to the central path.) For each value of $\Delta p/p_o$, the deviations of each of these points are added to r_o and r_o'. This gives a series of initial displacements for each value of $\Delta p/p_o$.

RESULTS

Radial Motion

Figure 5 gives the displacements, coming out of the D, of the centres of the radial phase ellipses for various momenta.

The graph of r_o against $\Delta p/p_o$ is a straight line up to $\Delta p/p_o = +0.5\%$. Above this the deviation is small (at $\Delta p/p_o = +1.65\%$ the deviation from the

straight line is + 0.125 cm). With $\Delta p/p_o$ as a percentage:

$$r_o = 9.595 + 1.175\ \Delta p/p_o \quad \text{cm} \qquad (7)$$

The plot of r'_o against $\Delta p/p_o$ is a gentle curve. If a straight line is taken between $\Delta p/p_o = \pm 1.65\%$ the maximum error is +1.05 mrad at $\Delta p/p_o = +0.25\%$. With this arrangement

$$r'_o = 40.450 + 3.667\ \Delta p/p_o \text{ mrad} \quad . \qquad (8)$$

Thus a linear momentum dispersion system in the beam transport would be adequate. However, from (8) and (9) the radial width of the beam at the F due to momentum spread $\pm$ 1.65% would be 8.22 cm (19.70 - 27.92 cm).

Passage through the D stray field does not destroy the elliptical distribution in phase space but makes the shape of the ellipse leaving the D strongly momentum dependent (see Figures 6, 7 for the extreme cases). The ellipses become more elongated with increase in momentum. There is also a tendency for particles which started on the surface of the original ellipse at the beginning of the D to accumulate at the extremes of the ellipses leaving the D.

Approximate parameters may be assigned to the ellipses leaving the D. If it was arranged that the incoming beam at the D should have those corresponding to the ellipse $\Delta p/p_o = 0$, the emittance would have to be increased to 3.64 cm . mrad to include all the ellipses $-1.65\% \leq \Delta p/p_o \leq 1.65\%$. However, computation of the common areas of the ellipses relative to that for $\Delta p/p_o = 0$ showed that if the emittance were kept at 2.3 cm.mrad, 93% of the beam coming within A = 2.3, $\Delta p/p_o = \pm 1.65\%$ would be accepted (see Figure 8). This may be reduced by a factor arising from the movement round the ellipse mentioned above.

The parameters of the ellipse $\Delta p/p_o = 0$ are (in the direction of the reversed beam)

$$\gamma = 7.775 \quad \text{mrad/cm}$$

$$\alpha = -1.655$$

$$\beta = 0.478 \text{ cm/mrad.}$$

Using the methods developed in EL/TM/14 this ellipse transformed back to the F magnet would have

$$\beta = 2.513 \text{ cm/mrad}$$

and the maximum radial extent would be $(2.3 \cdot 2.513)^{\frac{1}{2}} = 2.40$ cm. Thus at the F the minimum clearance of synchrotron orbit would be 17.30 cm and the radial extent of the beam 13.02 cm.

Vertical Motion

The vertical transfer matrix was calculated for each radial path above. Using these and the parameters of the vertical ellipse at the entrance to the D, the parameters of each vertical ellipse at the exit to the D could be calculated. For each momentum considered this gave 23 different sets of parameters, posing a problem for analysis.

This was approached as follows. Taking the vertical ellipse for the central path $\Delta p/p_o = 0$ as the standard:

1. the areas of the vertical ellipses for the central paths $-1.65 \leq \Delta p/p_o \leq +1.65\%$ common with the standard were calculated.
2. For each momentum the areas of the 22 vertical ellipses corresponding to the original points on the radial ellipse common with the standard were calculated and their mean value taken.

The results are shown in Figure 9. The mean common area over the momentum range in the central path calculation is 69%, that for the other case 67%. Thus it may be said that the vertical acceptance will be constant across the radial phase ellipse, and that if we define the vertical ellipse, at the D, of the incoming beam as the standard above, 68% of the beam with vertical emittance A = 2.3 cm.mrad will be accepted.

The parameters of the standard ellipse at the D are (in the direction of the reversed beam)

$$\gamma = 16.557 \text{ mrad/cm}$$
$$\alpha = 4.3318$$
$$\beta = 1.19375 \text{ cm/mrad.}$$

Thus there will be a cross-over at a distance

$$L = \frac{\alpha}{\gamma} = \frac{4.3318}{1.6557} = 2.62 \quad \text{m.}$$

beyond the D, i.e. 0.88 m before the F. The beam at the F will thus be diverging in both directions.

INFLECTOR IN LONG STRAIGHT

We calculate here the requirements of an inflector in the long straight which will give a clearance of the synchrotron orbit at the beginning of the F comparable to that obtained above with the inflector, inflection angle 20 mrad, in the short straight.

We take the minimum distance of the inflector from the D to be 50 cm. In the direction of the reversed beam the displaced equilibrium orbits are divergent in the long straight. At the F

$$\hat{x} = 1.9694 \text{ cm} / 1\%$$

$$\hat{x}' = 2.17 \text{ mrad} / 1\%.$$

Then clearance of the central path of the radial ellipse $\Delta p/p_o = -1.65\%$ at the F will be

$$r = \alpha \left\{ 300 - \ell/2 \right\} / \frac{p}{p_o} + 1.9694 \frac{\Delta p}{p_o} \text{ cm}$$

where α is the inflector angle (rad), ℓ the inflector length (cm) and $\Delta p/p_c$ a percentage. With an inflector length of 1m this becomes

$$r = 255 \alpha - 3.25 .$$

Now in the other inflector system this clearance would be 19.70 cm.

Thus for the same clearance we require

$$\alpha = \frac{19.70 + 3.25}{255}$$

$$= 0.09 \text{ rad.}$$

We take = 100 mrad. At the end of the inflector

$$\hat{x} = 1.5353 \text{ cm}/1\%$$

$$\beta_r = 0.721 \text{ cm/mrad.}$$

Thus good radial aperture required is

$$a = \frac{0.1 \cdot 50}{1.0165} + 1.5353 \cdot 1.65 + (0.721 \cdot 2.3)^{\frac{1}{2}}$$

$$= + \underline{8.725} \text{ cm} .$$

At the end of the inflector $\beta_v = 0.8681$ cm/mrad

but at the beginning $\beta_v = 1.220$ cm/mrad.

Thus vertical aperture required is

$$b = (1.22 \times 2.3)^{\frac{1}{2}}$$

$$= \underline{\pm 1.69} \text{ cm} .$$

At the F, displacement of central path

$$\Delta p/p_o = -1.65\% \text{ is } 22.25 \text{ cm}$$

displacement of central path

$$\Delta p/p_o = +1.65\% \text{ is } 27.86 \text{ cm}.$$

$\beta_r = 1.4290$ cm so maximum radial extent of beam due to betatron oscillations is $(2.3 \times 1.429)^{\frac{1}{2}} = 1.82$ cm.

Thus minimum clearance would be 20.43 cm with the radial extent of the beam 9.25 cm.

$\gamma_r = 4.0$ mrad/cm. Maximum divergence due to betatron oscillations is $(2.3 \times 4.0)^{\frac{1}{2}} = 3.15$ mrad. Thus divergence of beam at the F is $\pm$ 6.73 mrad ($\pm$ 3.58 from momentum spread, neglecting momentum dependent effect of the inflector).

For the vertical motion at the F α_v (in the direction of the reversed beam) is +0.7716 and $\gamma = 0.4$ rad/m. Thus there will be a cross-over at a distance

$$L = \frac{\alpha}{\gamma} = \frac{0.7716}{0.4} = 1.93 \text{ metres},$$

beyond the beginning of the F. At this point the perpendicular distance of the centre of the beam to the continuation of the synchrotron orbit in the long straight would be 44.3 cm, which together with the curvature of the magnet would give a clearance of over 50 cm over the synchrotron orbit in the F. (This neglects any curvature arising from the stray field of the F.)

CONCLUSION

It is apparent from the foregoing that the system with the inflector in the short straight has only one advantage, that pointed out in EL/TM/17, i.e. that the tolerances on the inflector switch-off do not need to be as tight as in the other system. The drawbacks of the short straight inflection are:

1) the decrease in acceptance due to passage through the D stray field
2) the difficulty of obtaining an inflector with a sufficiently good field when its transverse dimensions are comparable to its length
3) the extreme width and apertures required for beam equipment along the incoming beam.

TABLE I

Radial Range (cm)	(%/cm)	n
-4.8 to 4.8	-2.292	- 47.61
4.8 to 5.6	-2.50	- 51.93
5.6 to 5.9	-2.67	- 55.40
5.9 to 6.275	-3.20	- 66.48
6.275 to 6.8	-3.714	- 77.14
6.8 to 7.5	-4.50	- 93.48
7.5 to 8.0	-5.90	-122.60
8.0 to 9.0	-6.95	-144.40
9.0 to 11.0	-7.60	-157.90
11.0 to 12.0	-6.80	-141.30
12.0 to 12.5	-6.30	-130.80
12.5 to 14.0	-5.234	-108.70
14.0 to 14.675	-4.444	- 92.32
14.675 to 15.7	-3.806	- 79.05
15.7 to 17.5	-3.028	- 62.90

INFLECTION SYSTEMS

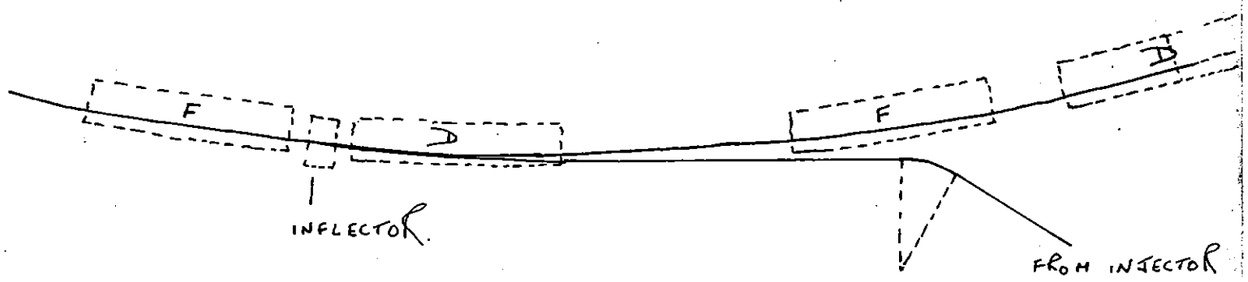

INFLECTOR IN SHORT STRAIGHT

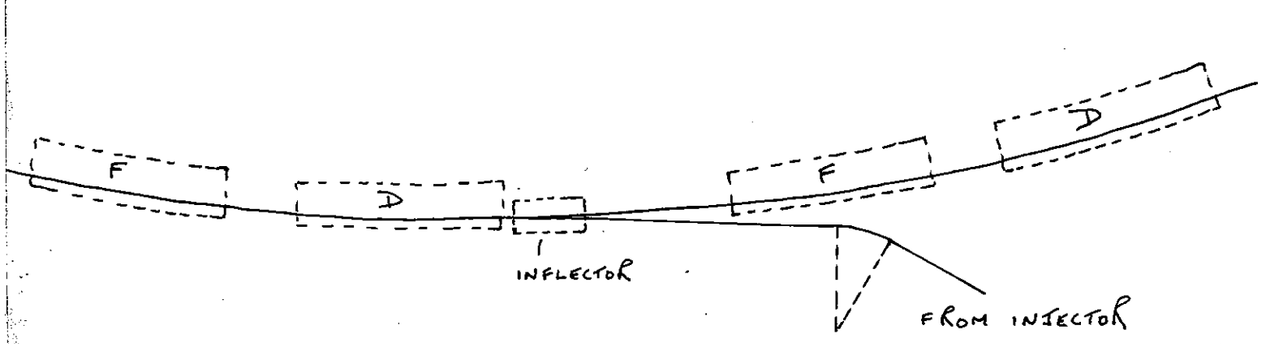

INFLECTOR IN LONG STRAIGHT

FIGURE 1.

METHOD FOR RADIAL PATH TRACING

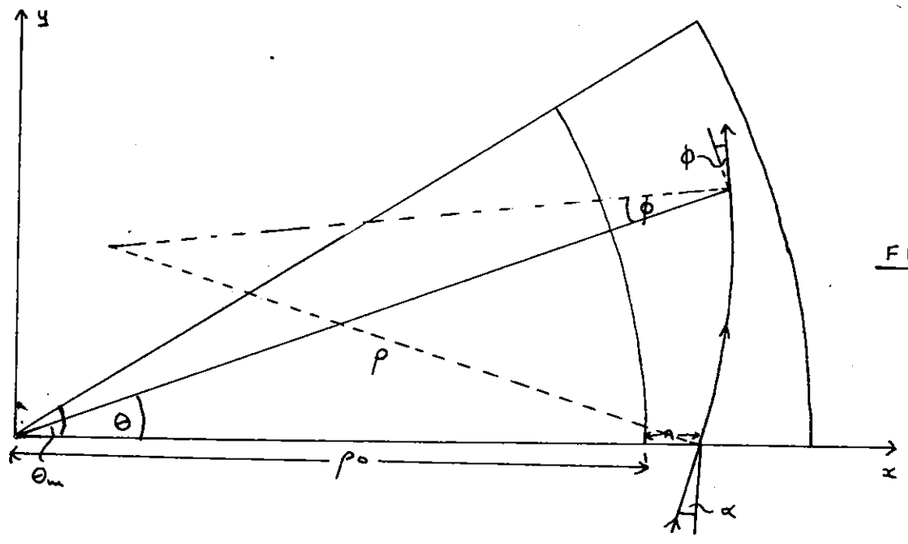

FIGURE 2.

Fig 3.

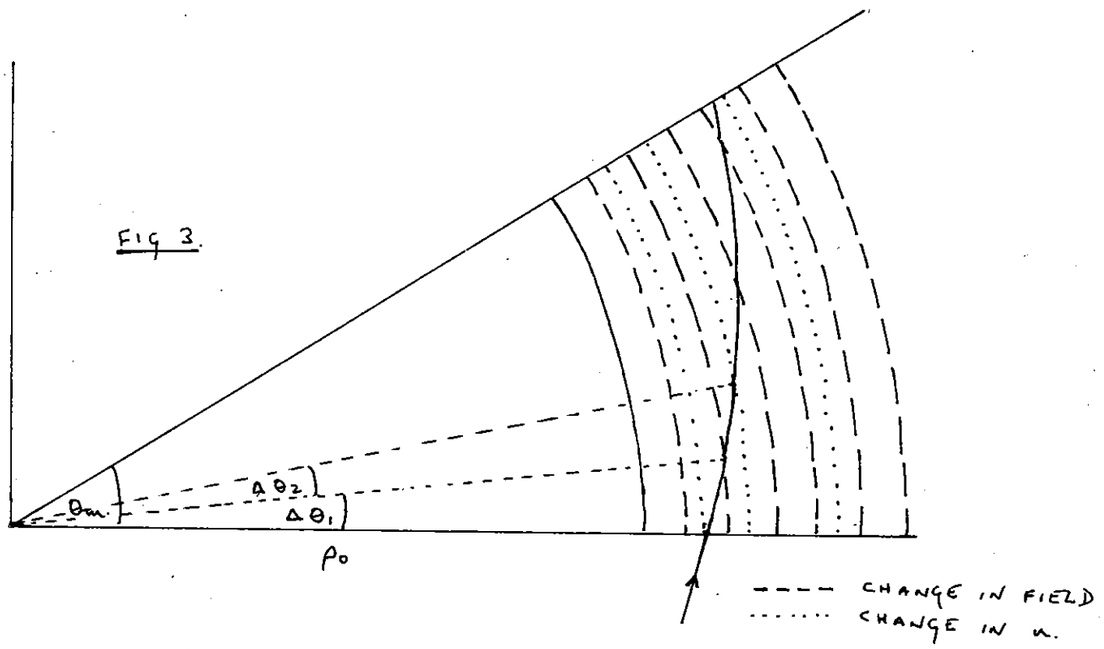

RADIAL PHASE ELLIPSE LEAVING D

$\frac{\Delta p}{p_0} = -1.65\%$

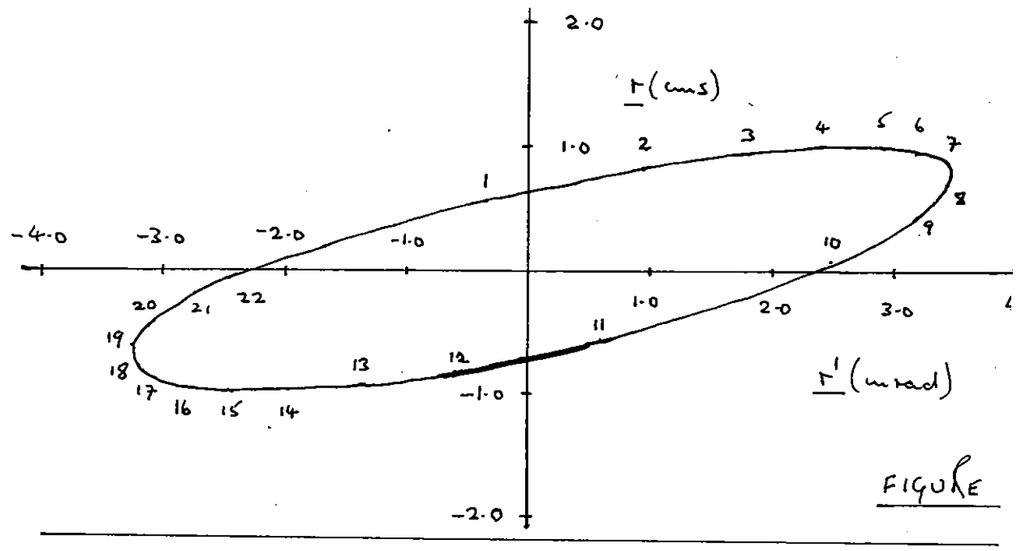

FIGURE

$\frac{\Delta p}{p_0} = +1.65\%$

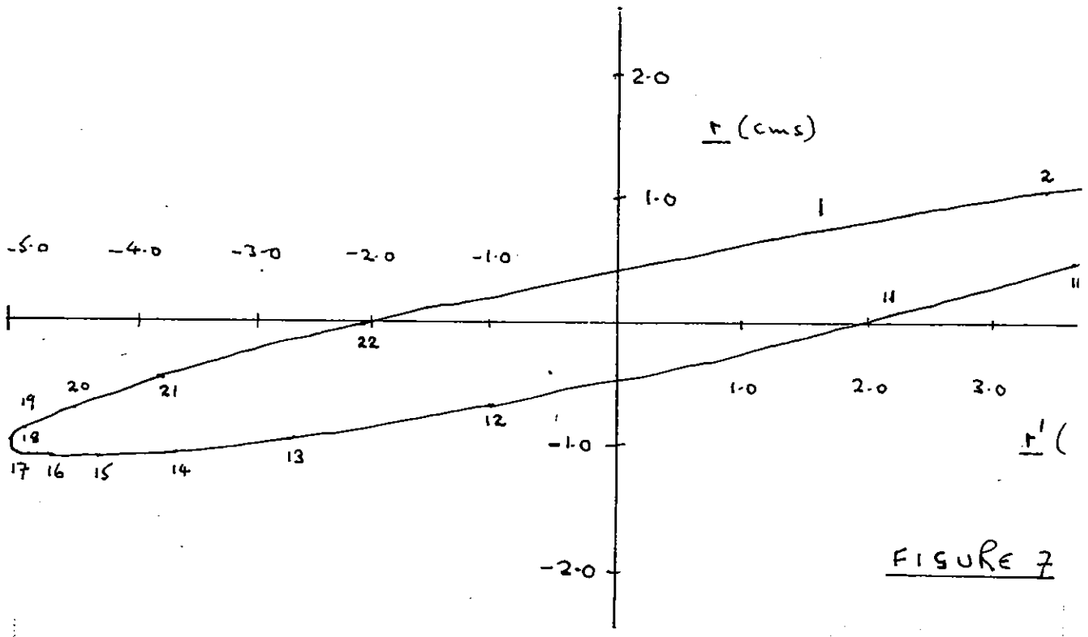

FIGURE 7

RADIAL PHASE ELLIPSE AT THE BEGINNING OF THE ⟩
(IN DIRECTION OF REVERSED BEAM)

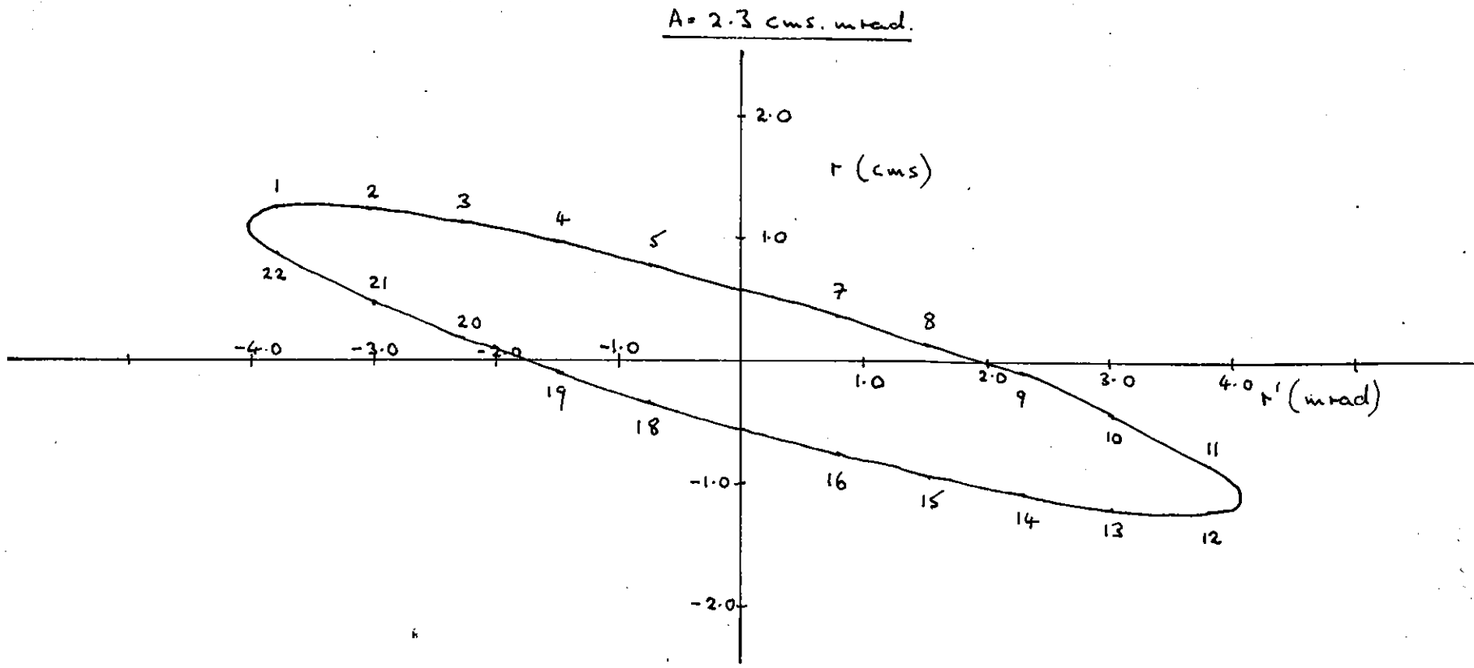

FIGURE 4

DISPERSION OF CENTRAL PATHS

(LEAVING THE D).

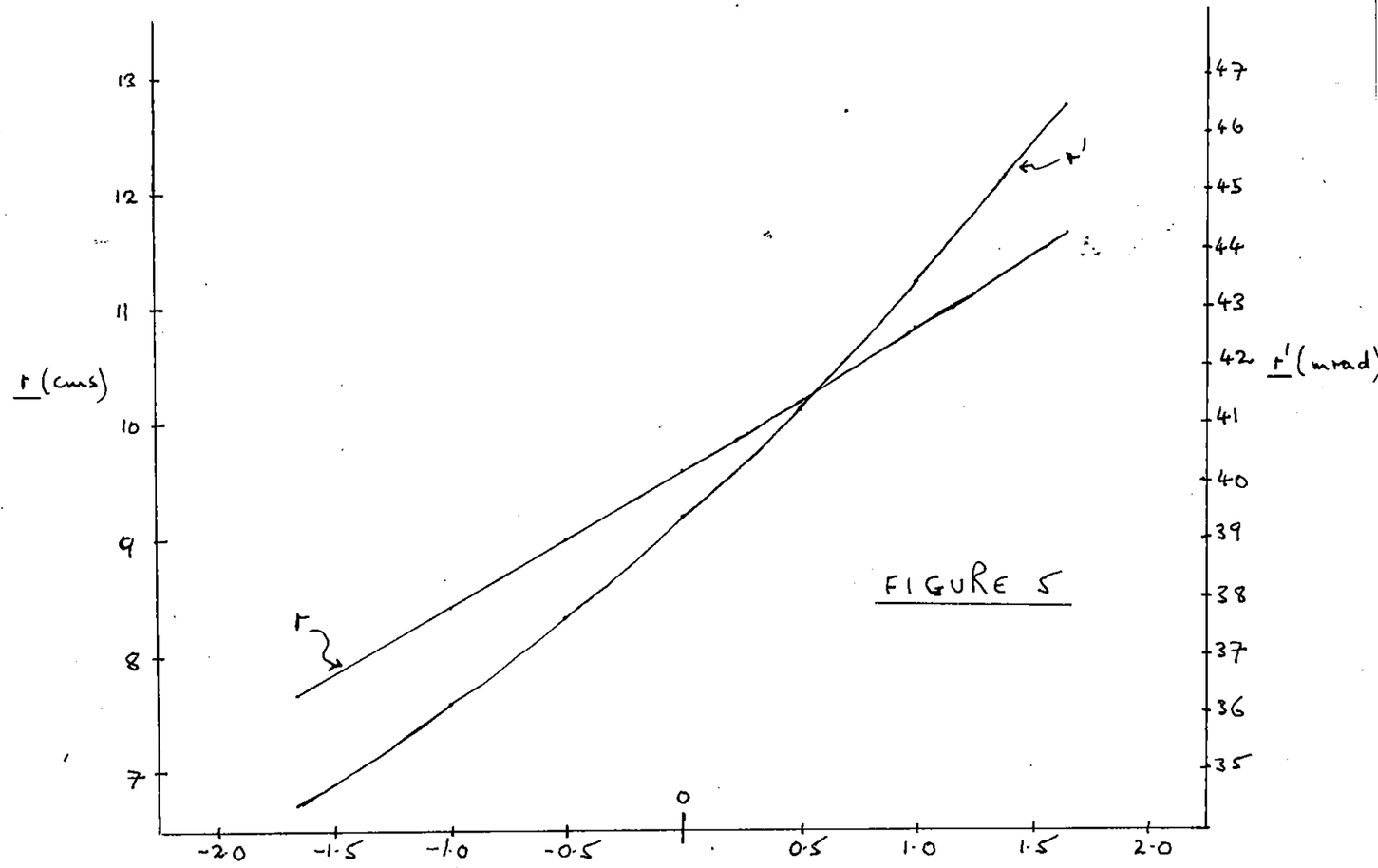

FIGURE 5

COMMON AREAS OF RADIAL ELLIPSES $-1.65\% < \frac{\Delta p}{p_0} < +1.65\%$ WITH ELLIPSE $\Delta p/p_0 = 0$

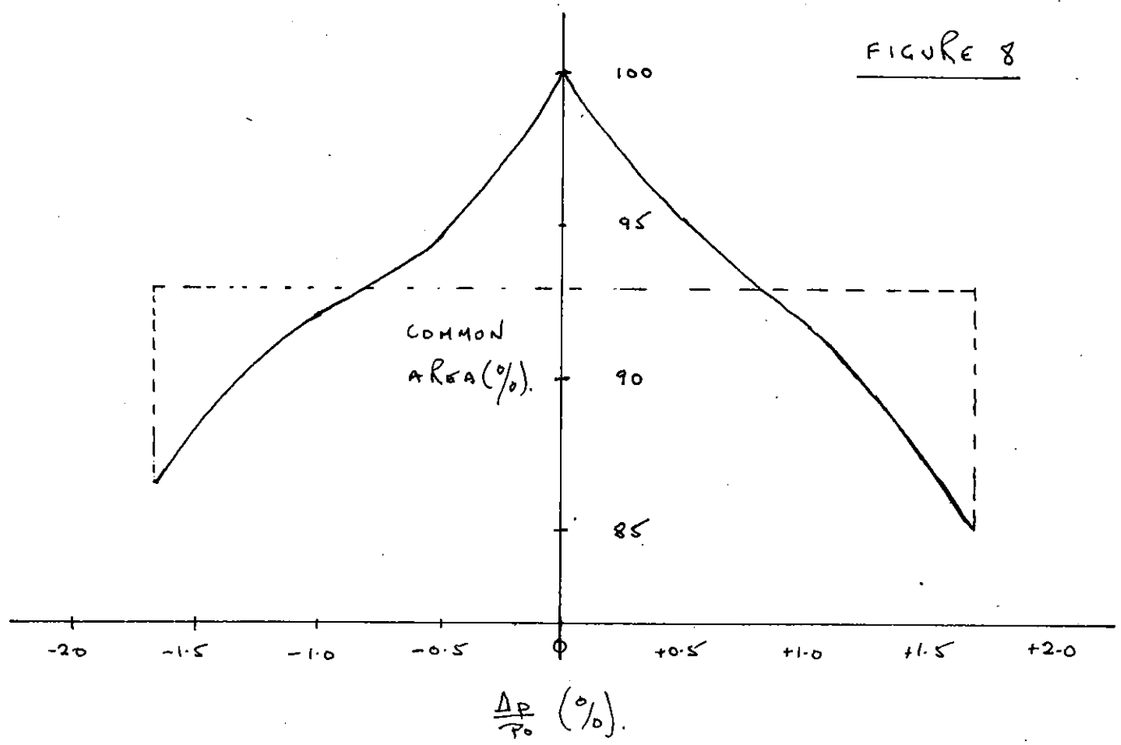

FIGURE 8